http://dx.doi.org/10.5516/NET.09.2013.103

DROP IMPACT ANALYSIS OF PLATE-TYPE FUEL ASSEMBLY IN RESEARCH REACTOR

HYUN-JUNG KIM*, JEONG-SIK YIM, BYUNG-HO LEE, JAE-YONG OH, and YOUNG-WOOK TAHK
Korea Atomic Energy Research Institute
Daedeok-daero 989-111, Yuseong-gu, Daejeon, Korea
*Corresponding author. E-mail : khj1392@gmail.com

Received December 06, 2013
Accepted for Publication March 14, 2014

In this research, a drop impact analysis of a fuel assembly in a research reactor is carried out to determine whether the fuel plate integrity is maintained in a drop accident. A fuel assembly drop accident is classified based on where the accident occurs, i.e., inside or outside the reactor, since each occasion results in a different impact load on the fuel assembly. An analysis procedure suitable for each drop situation is systematically established. For an accident occurring outside the reactor, the direct impact of a fuel assembly on the pool bottom is analyzed using implicit and explicit approaches. The effects of the key parameters, such as the impact velocity and structural damping ratios, are also studied. For an accident occurring inside the reactor, the falling fuel assembly may first hit the fixing bar at the upper part of the standing fuel assembly. To confirm the fuel plate integrity, a fracture of the fixing bar should be investigated, since the fixing bar plays a role in protecting the fuel plate from the external impact force. Through such an analysis, the suitability of an impact analysis procedure associated with the drop situation in the research reactor is shown.

KEYWORDS : Fuel Assembly, Drop Impact Analysis, Fuel Plate, Research Reactor, Structural Integrity

1. INTRODUCTION

In research reactors, the burned fuel assemblies are discharged, and the other fuel assemblies are shuffled by moving them to other positions according to the fuel management scheme. During the loading, unloading, and shuffling procedures, fuel assemblies are manipulated one by one using a handling system, and their movements are strictly limited to keep them under a certain water level in the pool to preclude the possibility of excessive radiation doses for workers. The postulated initiating events are referred to as unintended events that directly or indirectly endanger the fundamental safety functions, and they shall be selected appropriately for the purpose of analysis. The fuel assembly drop accident, which is classified as an erroneous handling, is regarded as one of the principal cause of the postulated initiating events to be considered in a reactor design [1]. In the IAEA safety standards series [2], mechanical damage to the core or fuel resulting from erroneous handling is considered as a postulated initiating event for research reactors. In the case of a drop accident during its transportation in a research reactor, a fuel assembly can be physically damaged to the point of releasing fission product into the environment. However, in reality, fuel plates are put in place inside the fuel assembly and thus are unlikely to be mechanically damaged by the collision between fuel assemblies or structures, and therefore damage related radiation product release is rarely conceivable. Nonetheless, a fuel assembly drop accident shall be considered in the reactor design to show that the release of radioactive products from an accident will not cause severe radiological consequences therefrom. In the present work, the impact behavior of a fuel assembly is investigated so that the number of failed fuel plates shall not exceed the figures for the calculation of fission gas release in the dose analysis in the reactor building.

There have been some studies on fuel assembly drop accidents used in a power reactor. Wu et al. [3] considered the BWR (Boiling Water Reactor) drop events in which the fuel assembly drops onto the pool bottom. The fuel structural integrity is investigated through a stress calculation. Namgung et al. [4] performed an RV (Reactor vessel) head drop analysis on the reactor core used in a KSNP+ (Improved Korean Standard Nuclear Power Plant). Three RV drop scenarios are considered, and it is shown that the reactor core remains in a coolable state. Petkevich et al. [5] simulates the PWR (Pressurized Water

Reactor) fuel assembly drops during transportation. Yim et al. [6] evaluates the fuel plate integrity during a fuel assembly drop accident using an energy method.

However, there has been no systematic research of a fuel assembly drop accident in a research reactor with full consideration of various possible scenarios, such as a fuel assembly drop on the standing fuel assemblies. From the viewpoint of drop impact behavior on the fuel assembly, a drop accident can basically be categorized into two scenarios based on where the drop accident occurs, outside or inside the reactor. For the former case, the fuel assembly may drop onto the pool bottom or other mechanical components lying in the service pool. For the latter case, the falling fuel assembly may drop onto the loaded fuel assembly standing on the core.

The purpose of the present work is to check whether a fuel plate failure may occur under the drop situations in a research reactor, and how the impact force will influence the fuel plates. The impact analysis procedure suitable for each situation is established, and an appropriate analysis model is constructed, reflecting the dynamic behavior to be expected. The fuel assembly drop impact analysis is basically carried out using the explicit analysis code of LS-DYNA [7]. However, an implicit analysis using ANSYS [8] is also utilized if possible, and the results are compared to those of an explicit analysis.

This paper is organized as follows. In section 2, the overall analysis methodology is explained. Brief descriptions of a plate-type fuel assembly, classification of fuel assembly drop accidents and the impact velocity calculations are presented. In section 3, the impact analysis results are shown. The stress calculation of the fuel plate and the fracture mechanism are presented. In section 4, some concluding remarks are presented.

2. ANALYSIS MODEL AND PROCEDURES

The drop impact problem in the pool is basically a fluid-structure interaction problem. The coupled computational structural analysis and CFD (computational fluid dynamics) analysis are required. However, since the computational costs are very high in this approach, the following sequential analysis approach has been used in many drop impact analyses. The impact velocity is first computed when the fuel assembly freely falls in a water environment. The structural analysis is then performed with the assumption that the fuel assembly impacts an object at impact velocity in the air environment. This is a conservative method from a stress point of view, because the fluid resistance at the moment of impact is omitted in the air environment. In this section, a brief description of the fuel assembly, a classification of the drop accident, and a computation of the impact velocity are presented. A numerical analysis procedure suitable for each drop case is then constructed and performed.

2.1 Brief Description of Fuel Assembly for Research Reactor

Whereas the PWR fuel assembly is large about four and five meters high and weighs about half a tonne, the research reactor uses a plate-type fuel element that is small size and lightweight compared to that of a PWR. Unlike power reactors, research reactors operate with the much higher power density necessary to achieve high neutron fluxes. For this reason, its fuel is usually in the form of a metal plate covered by aluminum. These are very different from the fuel rods with ceramic pellets used in the power reactors. From the international program of the RERTR (Reduced Enrichment in Research and Test Reactors) initiated by the U.S. Department of Energy in 1978, many research reactors that were using HEU (high-enriched uranium) started to gradually convert their cores to use LEU (low-enriched uranium) (less than 20 wt% ^{235}U) fuel. Under this program, more than 40 research reactors have been converted.

KAERI (Korea Atomic Energy Research Institute) designed a plate-type fuel assembly to be used in a research reactor, which is shown in Fig. 1. The plate-type fuel, which has almost been standardized, is used in many research reactors. Fig. 2 shows the fuel assembly configuration. The fuel assembly contains 21 fuel plates. Each fuel plate is composed of fuel meat hermetically sealed in and rigidly bonded to its cladding for structural integrity. The fuel meat is made of a fine and homogeneous dispersion of U_3Si_2 particles in a continuous aluminum matrix. The fuel is LEU with a ^{235}U enrichment of 19.75wt%. This U_3Si_2-Al dispersion fuel up to a uranium density of 4.8gU/cm^3 was qualified by the U.S. Nuclear Regulatory Commission [9] in 1988. Considerable experiences in irradiation performance and manufacturing have been accumulated on U_3Si_2-Al fuel in research and test reactors. In this regard, U_3Si_2-Al dispersion fuel is presently considered the best-qualified fuel in terms of uranium loading and performance in research reactors. In the manufacturing process, the fuel plates are assembled one after another between two-grooved side plates, and then attached firmly by applying plastic deformation on

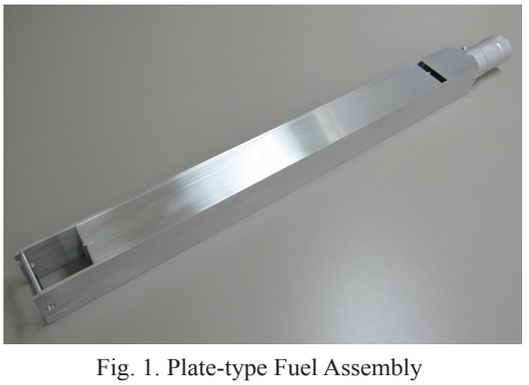

Fig. 1. Plate-type Fuel Assembly

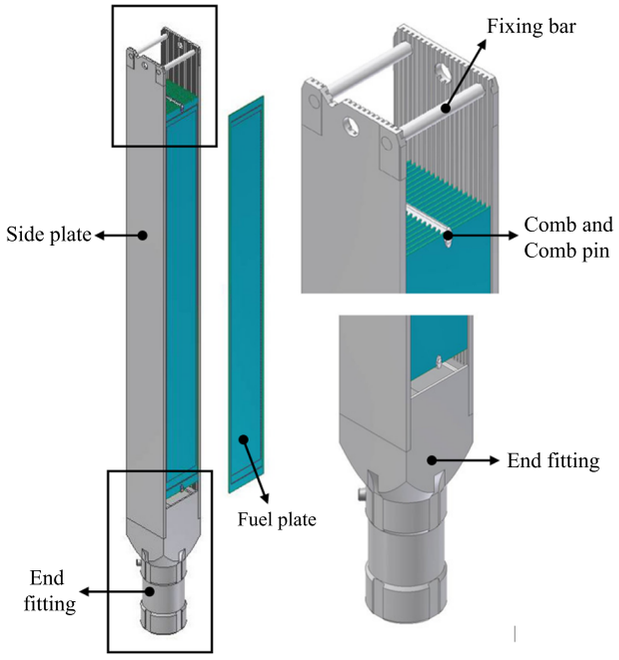

Fig. 2. Configuration of Plate-type Fuel Assembly

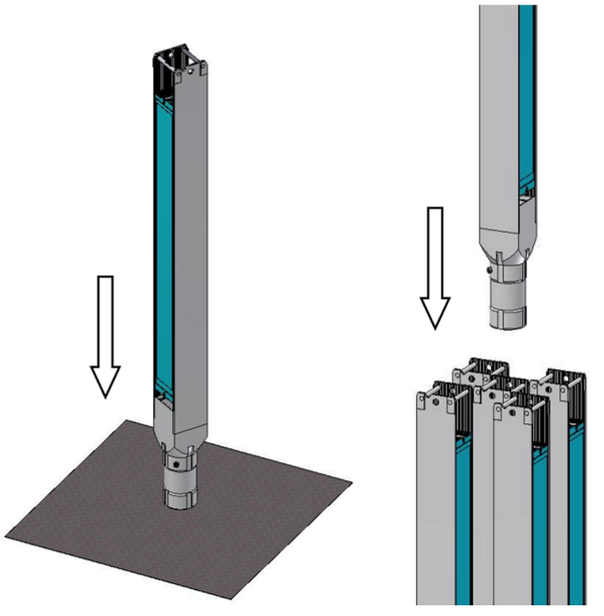

Fig. 3. Drop Accident Cases: (a) Fuel Assembly Drop onto the Pool Bottom, and (b) Fuel Assembly Drop onto the Loaded Fuel Assembly Bundles

the crests between the grooves, by means of roll-swaging. The assembled fuel plates are structurally reinforced at both the upper and lower ends by two sets of combs and comb pins. At the top of the fuel assembly, the two cylindrical rod-shaped fixing bars are connected, to maintain the spacing the side plates. The bottom end fitting is jointed to side plates by welding. All of the fuel assembly component material, except the fuel plates, is aluminum alloy 6061-T6, in order to provide its high strength and good performance in a reactor core. When the fuel assembly is loaded in the core, the lower cylindrical part of the end fitting is inserted into the fuel hole on the grid plate, and the fuel assembly can then stand alone in its position without any lateral support.

2.2 Classification of Drop Accidents and their Maximum Drop Height

For the first scenario, a drop accident occurring inside the reactor, the direct drops onto the pool bottom is considered. By taking into account the fact that the pool bottom has an almost rigid property, and the maximum impact velocity is achieved at the moment of impact, a direct impact with pool bottom, as shown in Fig. 3(a), is regarded as the most severe impact case. Two different analysis approaches to this scenario, implicit and explicit, are used and their results are compared. The depth of the pool in which the fuel assemblies are operated is assumed to be 10 m. According to KAERI's design, whenever a fuel assembly is handled, it is thoroughly restricted to remain beyond 3.9 m below the water surface, to preclude excessive dose to workers. Considering the length of the fuel assembly, 1.015 m, the maximum drop height becomes 5.085 m outside the reactor.

The second scenario is described in Fig. 3(b): a drop onto the loaded fuel assembly bundles. In such case, the bottom part of the falling fuel assembly, the end fitting, can first hit the fixing bar located on the top of the standing fuel assembly. It may subsequently damage the fuel plates of the standing fuel assembly if the fixing bar is fractured. If the fixing bar withstands a fracture, it can be concluded that the fuel plates remain intact, because the fixing bar protects the fuel plates from direct impact. It is therefore important to check whether a fracture of the fixing bar occurs. The fuel assemblies are loaded onto a grid plate in the reactor structure, and the grid plates are located 1.925 m above the pool bottom in the KAERI designed research reactor. Thus, the maximum drop height becomes 3.160 m inside the reactor.

There can be many falling modes when the fuel assembly drops. The fuel assembly can drop with various inclined angles due to an unanticipated external fluid force, collision with other components during a drop, and so on. When the fuel assembly drops vertically, the drag force caused from the fluid resistance reaches the smallest possible value, which results in the maximum impact force. Among the various falling modes, the vertical drop case is considered as the most severe case from an impact point of view.

2.3 Design Criteria

The acceptance criteria for safety should be developed in accordance with the reactor conditions. The events of

the reactor operation are generally classified into normal operation condition, anticipated operational occurrences, accident condition, and limiting accident condition, in accordance with the estimated occurrence frequency and their radiological consequences. Normal operation pertains to nominal operational conditions including a start-up, power operation, shutdown, maintenance, and refueling. An anticipated operational occurence is an event expected to occur more than once during the lifetime of a reactor. The accidents and limiting accidents are events that are not expected during the lifetime of the reactor, but are defined for the reactor design. The event frequencies of the accidents are estimated to be greater than those of limiting accidents. Following the recent practices of research reactors, PWRs, and the IAEA safety series report [1, 10], the limiting accidents are not expected to occur, but are postulated in the design. Since a drop accident is considered as a postulated accident event and is regarded as an event unlikely to occur, the design criteria of the Level D service limits described in the ASME Section III, 2004 edition [11] are used as a general guide in the evaluation of structural behaviors of a fuel assembly. These sets of limits permit gross general deformations with some consequent loss of dimensional stability and damage requiring repair, which may require the removal of the component or service support. The design criteria of ASME section III are based on the maximum shear stress theory (Tresca criterion), and the design stress intensity value, S_m, which becomes the allowable limit, is defined for the structural integrity, which forms the basis for the stress limit. The stress intensity limit shall be less than $2.4S_m$ or $0.7S_u$ for primary membrane stress, and $3.6S_m$ or $1.05S_u$, for primary membrane stress plus primary bending stress. S_u is the ultimate tensile strength. Table 1 summarizes the stress limits of the drop impact analysis.

2.4 Impact Velocity Calculation

During the free fall, the forces exerted on the fuel assembly are weight, buoyancy, and drag. From Newton's second law of motion, the governing equation is written as

$$\left(m-\rho V\right)g-F=\left(m+m_a\right)\frac{dv}{dt}, \tag{1}$$

where m_a is the added mass on the fuel assembly, t is time, V is the fuel assembly volume, g is the acceleration of gravity, and F is the drag force. The submerged weight of the fuel assembly is $(m-\rho V)g$. In fluid dynamics, the drag equation is a practical formula used to calculate the drag force owing to movement through a fully enclosing fluid. The drag force is written as

$$F=\frac{1}{2}\rho AC_D v^2, \tag{2}$$

where C_D is the drag coefficient, ρ is the fluid density, v is the fuel assembly velocity, and A is the orthographic projection of the fuel assembly on a plane perpendicular to the direction of motion. As the velocity of the fuel assembly increases, the resisting drag force also increases. The differential equation (1) is rearranged as

$$\int_0^v \frac{dv}{(m-\rho V)g-\frac{1}{2}\rho AC_D v^2}=\frac{1}{m+m_a}\int_0^t dt \tag{3}$$

Solving this differential equation, the velocity becomes

$$v=\sqrt{\frac{(m-\rho V)g}{\frac{1}{2}\rho AC_D}}\tanh\left(t\frac{\sqrt{(m-\rho V)g\cdot\frac{1}{2}\rho AC_D}}{m+m_a}\right) \tag{4}$$

Equation (4) is an analytical solution of the terminal velocity, which considers the weight, buoyancy, and drag forces.

The fuel assembly accelerates until the gravitational force balances the resistance forces created by the fluid. At this time, the fuel assembly has reached its maximum kinetic energy, and consequently its terminal velocity. Since the acceleration herein is zero, the terminal velocity is then [12, 13]

$$v_t=\sqrt{\frac{(m-\rho V)g}{\frac{1}{2}\rho AC_D}} \tag{5}$$

Although the precise CFD calculation accompanying the experiment might be required to obtain the drop impact velocity of the fuel assembly, the impact velocity is simply computed under the assumption using the drag coefficient in reference [14]. It is shown that the drag coefficient of

Table 1. Stress Limit for Drop Impact Analysis

Design limit	Components	Stress limit
$P_m < \text{Min}(2.4S_m \text{ or } 0.7S_u)$ $P_m + P_b < \text{Min}(3.6S_m \text{ or } 1.05S_u)$	Fuel plate	$P_m < 126\text{MPa}$ $P_m + P_b < 189\text{MPa}$
	Structural component except fuel plate (aluminum alloy 6061-T6)	$P_m < 203\text{MPa}$ $P_m + P_b < 305\text{MPa}$

※ P_m: membrane stress, P_b: bending stress, S_m: design stress intensity, S_u: ultimate tensile strength

a cylindrical structure is at least larger than 0.8 for various length/diameter ratios. Thus, a drag coefficient of 0.8 is used. The geometric properties of the plate-type fuel assembly designed by KAERI are as summarized in table 2. From equation (5), the fuel assembly terminal velocity is calculated as 5.36 m/s. The highest attainable impact velocity of fuel assembly becomes 4.58 m/s and 4.0 m/s for accidents occurring outside and inside the reactor, respectively. For both accident cases, the falling fuel assembly impacts before reaching terminal velocity.

2.5 Implicit and Explicit Analyses

In the field of solid mechanics, specifically for nonlinear problems, a finite element equation solution method can be classified into two distinct categories: implicit and explicit algorithms.

An explicit analysis does the incremental procedure, and the stiffness matrix based on the geometry or material changes is updated at the end of each increment. An incremental solution of the system is then derived from a newly constructed stiffness matrix. In this analysis, if the increments are small enough, the results will be accurate. If the number of increments is not sufficient, the solutions tend to drift from the correct solution. Thus, the explicit approach has a drawback in that it is conditionally stable. The stability limit for the explicit integration operator is that the maximum time increment must be less than the critical value of the smallest transition times for a dilatational wave to cross any element in the mesh.

An implicit analysis is the same as an explicit one, with the addition that after the increment the analysis conducts Newton-Raphson iterations to enforce the equilibrium of the internal structure forces with the externally applied loads. This type of analysis tends to be more accurate and can take larger increment steps. The drawback of an implicit analysis is that during the Newton-Raphson iterations, one must update and reconstruct the stiffness matrix for each iteration. It encounters numerical difficulties in converging to a correct solution during an analysis involving large deformations, highly nonlinear plasticity, and contacts. The computational cost in the tangent stiffness matrix is dramatically increased, even causing a divergence. However, for an explicit approach, the computation time is approximately proportional to the size of the finite element model, and does not change as dramatically as with the implicit approach. Thus, an explicit dynamics analysis is generally used to determine the dynamic response of a structure owing to stress wave propagation, impact, or rapidly changing time-dependent loads. The explicit integration operator is conditionally stable, and thus the time increments must satisfy

$$\Delta t \le \frac{2}{w_{\max}}, \tag{6}$$

where $w_{\max}$ is the element maximum eigenvalue. A conservative estimate of the stable time increment is given by the minimum value for all elements. The above stability limit can be written as $\Delta t = 0.9\ I / c$, where I is the characteristic length, and c is the wave propagation velocity, which are dependent on the element type. For stability, a scale factor of 0.9 is used to decrease the time step in LS DYNA [7].

Table 2. Geometric Properties of Plate-type Fuel Assembly Designed by KAERI

Properties	Value
Weight	7.5kg
Length	1.015m
Volume	2166.7cm^3
Water density (40ºC)	992.25kg/m^3
Projected area	46.13cm^2
Buoyancy force	2.15kg
Fuel plate dimension	70.7 mm x 1.27 mm x 680 mm
Fuel assembly envelope	76.2 mm x 76.2mm x 1015 mm

2.6 Contact Algorithm

The efficient and robust solution to contact problems mainly relies on, besides a good discretization of the contact interface, the algorithms. Algorithms that are applied in many standard finite element programs are related either to a penalty method or to the Lagrange multiplier method.

The penalty method uses a contact spring to establish a relationship between the two contact surfaces. The spring stiffness is called the contact stiffness. The augmented Lagrangian method is an iterative series of the penalty method. The contact tractions are augmented during equilibrium iterations so that the final penetration is smaller than the allowable tolerance. Compared to the penalty method, the augmented Lagrangian method usually leads to better conditioning and is less sensitive to the magnitude of the contact stiffness, especially for the problem in which the mesh becomes distorted. The pure Lagrange multiplier method adds contact traction to the model employing additional degrees of freedom, λ. The pure Lagrange multiplier method does not require contact stiffness. This method adds contact traction to the model as additional degrees of freedom, and requires additional iterations to stabilize the contact conditions. It often increases the computational cost compared to the augmented Lagrangian method. For further details of the contact algorithm, refer to [15].

In the implicit analysis of ANSYS, the augmented Lagrange method is adopted as a contact algorithm. The normal contact stiffness is affected by the defined material properties, element size, and the total number of degrees

of freedom in the model. In the explicit method of LS-DYNA, a contact algorithm based on the penalty parameter is used. In the LS-DYNA, the contact stiffness, k, is determined by the following relationships.

$$k = \frac{f A^2 K}{V}, \tag{7}$$

where f is the penalty factor, A is area of contact segment, K is the bulk modulus of the contact element, and V is the volume.

2.7 Plastic-kinematic Hardening Model

The plastic-kinematic hardening model is a strain-rate dependent elastic-plastic model. In the explicit analysis, the Cowper-Symonds model [7, 16], which provides a multilinear elastic-plastic stress strain relation, is used. The Cowper-Symonds material model is a simple elasto-plastic, strain-hardening model that uses the empirical formulation described by Ludwik [17], in which materials strengthen when plastic deformations are applied. A multilinear elastic-plastic model is a very commonly used plasticity law, especially for steel. The strain rate accounted for in the Cowper-Symonds model, which scales the yield stress by the strain rate dependent factor, is shown below.

$$\sigma_Y = \left(1 + \left(\dot{\varepsilon} / C\right)^{1/P}\right)\sigma_0 \tag{8}$$

where σ_Y is the dynamic yield stress, σ_0 is the yield stress without considering the strain rate, $\dot{\varepsilon}$ is the effective strain rate, and C and P are the Cowper-Symonds strain rate parameters. Using this model, the true stress – true strain curve of aluminum alloy 6061-T6 becomes like that in Fig. 4. A higher dynamic yield strength is obtained in which the higher strain rate is observed.

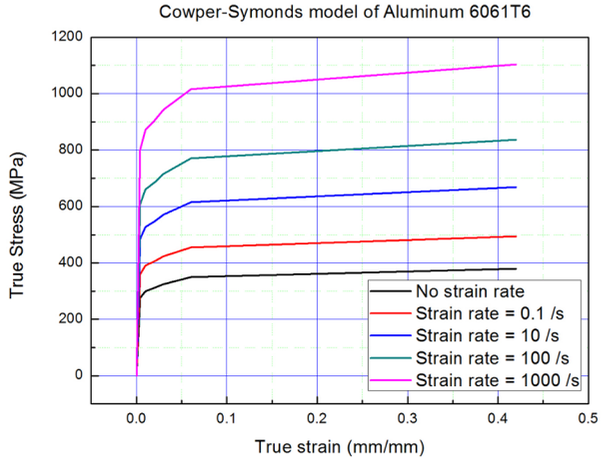

Fig. 4. Stress-strain Relation of Aluminum Alloy 6061-T6

3. FINITE ELEMENT ANALYSIS OF FUEL ASSEMBLY DROP ACCIDENT

As was discussed in section 2.2, the drop accident can be classified into two situations. In the present work, a finite element modeling and analysis strategy are constructed for each case.

3.1 Fuel Assembly Drop Accident Occurring Outside of the Reactor: Drop onto the Pool Bottom

For a drop accident occurring outside the reactor, the dropped fuel assembly may directly impact the pool bottom or the other mechanical components. If the fuel assembly drops and impacts other structures, it is likely to be physically damaged. Since most of the shock may be absorbed by the end fitting of the fuel assembly, the fuel plates may only be slightly bent or mechanically damaged. A quantitative assessment on how much the fuel plate is damaged is required for an assessment of the fission product release. In this regard, the stress of the fuel plate is calculated under the impact condition, and is compared with the design criteria of the ASME Code [11]. Since it is expected that the failure behavior of the fuel assembly is not too much, two different analysis approaches, implicit and explicit, are carried out, and their results, such as stress and contact force, are compared.

3.1.1 Finite Element Model

The fuel assembly at the moment of impact is modeled using finite element meshes, as shown in Fig. 5. The fuel assembly and pool bottom are modeled so that they are sufficiently close to each other. The pool bottom is coarsely

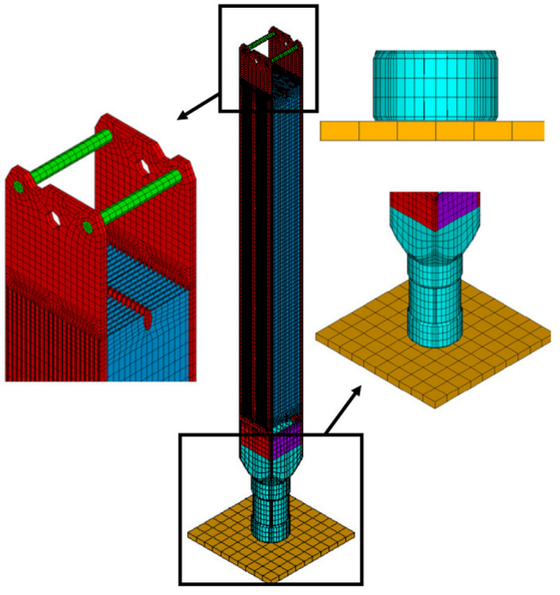

Fig. 5. Finite Element Model of Fuel Assembly at the Moment of Impact

modeled with high stiffness. Then, an initial impact velocity of 4.58m/s is imposed on the fuel assembly as initial condition. The total numbers of nodes and elements are 180,313 and 136,313. Contact surfaces should have been designated by contact elements before the analysis. The elements of Conta173 and Targe170 in ANSYS form a contact pair. The geometric nonlinear effect is considered. For the friction coefficient, 0.1 is assumed. It should be noted that the contact is represented differently in an explicit dynamic analysis than it is in other types of ANSYS analyses. For explicit dynamics such as LS-DYNA, there is no specific contact element. Simple indication of the contact surfaces and the type of contact between them are just necessary.

3.1.2 Analysis Results

In engineering applications, a stress analysis is usually important to analyze and predict a failure. Fig. 6 shows the stress intensity history of the fuel assembly resulting from ANSYS. As the impact starts, the stress is concentrated at the bottom tip at the moment of impact, and then propagates throughout the body and diffuses away over time.

Fig. 7 shows the maximum stress history at the cladding of the fuel plate, and Fig. 8 shows the contact force over time. The maximum stress at the fuel plate is around 120MPa, which is lower than the design limit of 189MPa for the accident case. Thus, it is expected that the fuel plate structural integrity will be ensured. In the impact analysis, as in the rest of the analyses shown in this paper, only the first impact phenomenon is considered and analyzed. The subsequent impact is not simulated, since the first impact is the dominant ingredient for a structural integrity evaluation. The stress oscillation in the graph is due to wave propagation and attenuation, not to additional impact. Comparisons between explicit and implicit methods are also made in the figures. The graphs show that the patterns of stress distribution and contact force are similar for most regions. The explicit analysis results follow well with those of the implicit analysis. Although there is a slight delay on the profiles between the two

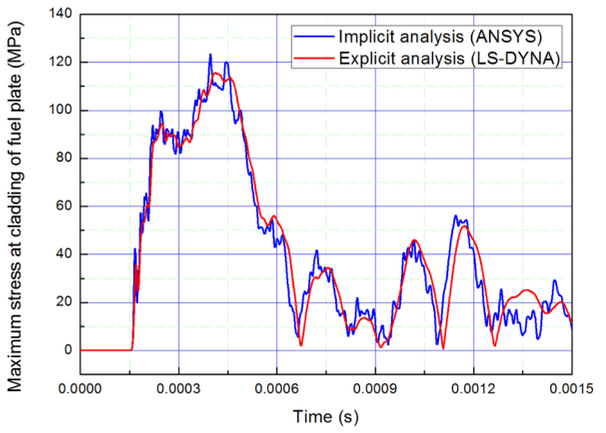

Fig. 7. Maximum Stress History at Cladding of Fuel Plate

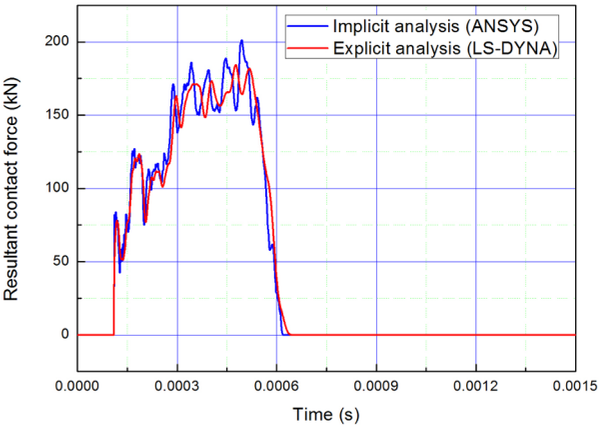

Fig. 8. Contact Force History

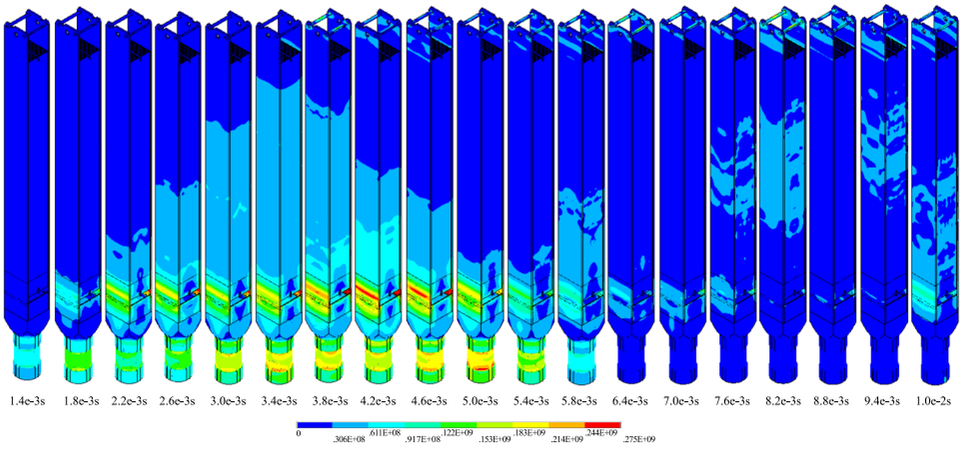

Fig. 6. Stress Distribution History from Implicit Analysis

methods, this slight discrepancy is acceptable. It is observed that the values of the implicit methods oscillate more than those by the explicit analysis. When solving the problem using the implicit method, the CPU time significantly increases. Table 3 shows a comparison of the analysis time. The analysis time of the explicit method is 47.5 min (2853 s), while that of the implicit method is 44.3 hr (159389 s). The CPU time of the explicit analysis is 56-times faster than that of the implicit analysis, since the explicit analysis passes to the next state without the equilibrium procedure between the internal and external forces by the Newton-Raphson iteration.

More studies on the different impact velocity and structural damping ratios were performed. Figs. 9 and 10 are the results by varying the impact velocity. Four different impact velocities, 1.5 m/s, 2.5 m/s, 3.5 m/s, and 4.58 m/s, are used for the analysis. As the impact velocity increases, the impact start time becomes shorter and the magnitude of stress and contact force increases.

Motion in a structural system will dissipate energy due to structural damping, which is caused by internal friction within the material or at connections between elements of a structural system. Four structural damping ratios, 0%, 3%, 5%, and 10%, are used for the study. For imposing the structural damping to the fuel assembly, the proportional damping model, in which the damping force vector

Table 3. Comparison of Analysis CPU Time between Implicit and Explicit Approaches

Analysis type	Time
Implicit approach (ANSYS)	159389 sec (44.3 hours)
Explicit approach (ANSYS LS-DYNA)	2853 sec (47.5minutes)
Computer performance: Intel core i7 CPU, 3.2GHz, 24GB Ram, Windows 7 (64bit)	

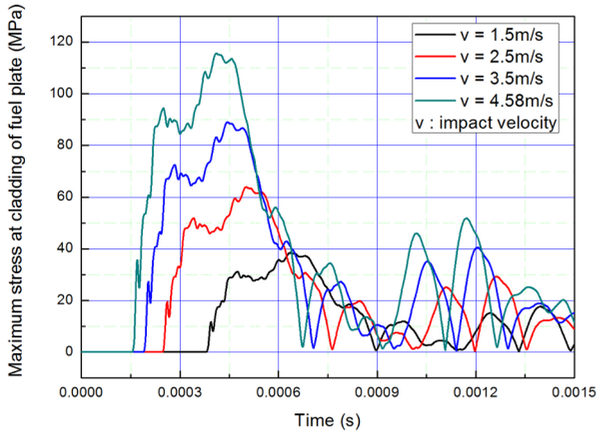

Fig. 9. Maximum Stress History at Cladding of Fuel Plate with Respect to Impact Velocities

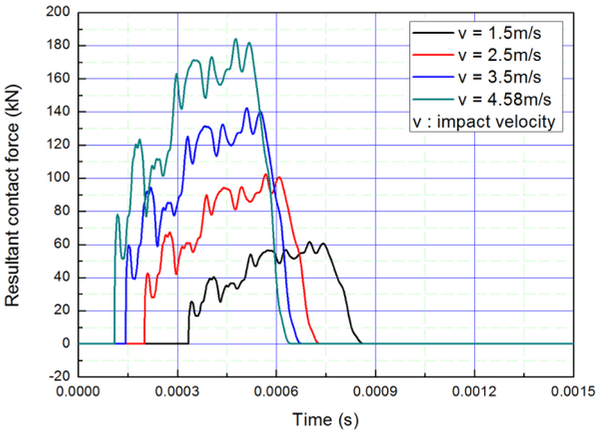

Fig. 10. Contact Force History with Respect to Impact Velocities

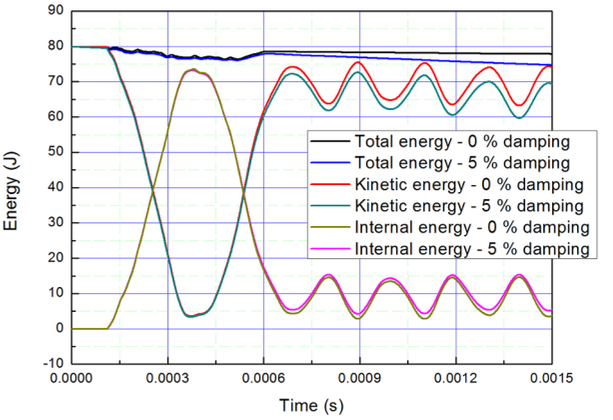

Fig. 11. Total, Kinetic, and Internal Energy History with Respect to Structural Damping Ratios

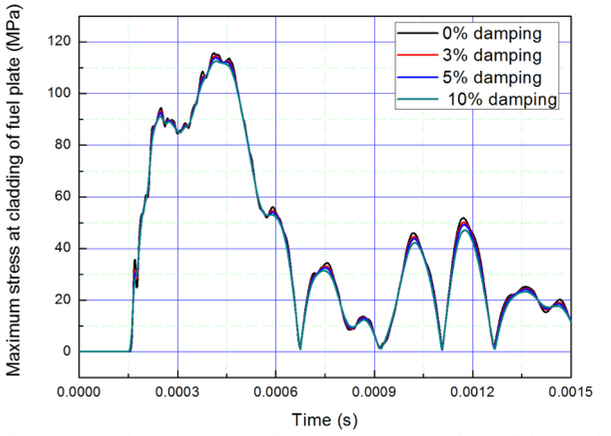

Fig. 12. Maximum Stress History at the Cladding of the Fuel Plate with Respect to the Structural Damping Ratios

is proportional to a linear combination of the mass and stiffness matrix, is used. Fig. 11 is the total, kinetic, and internal energy history of the 0% and 5% damping ratio, and Figs. 12 and 13 are the stress and contact force profiles

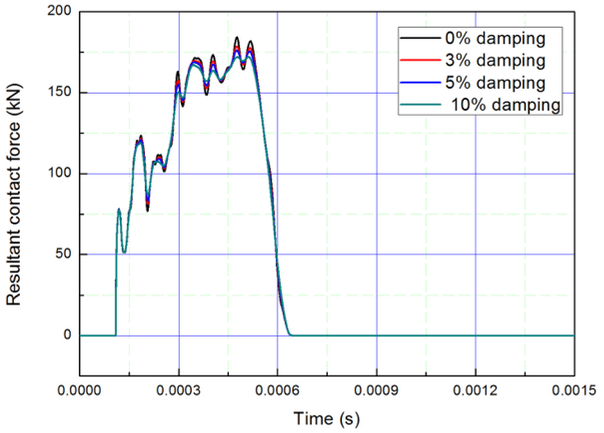

Fig. 13. Contact Force History with Respect to the Structural Damping Ratios

of four different damping ratios. As the damping ratio increases, more shock energy is dissipated, and less deviation of the stress is enjoyed.

In summary, even though the drop accident occurs outside the reactor at a certain attainable maximum drop height, the structural integrity of the fuel plate is maintained.

3.2 Fuel Assembly Drop Accident Occurring Inside the Reactor: Drop onto the Reactor Core

During the fuel assembly loading and discharging procedures in the reactor core, the fuel assembly may inadvertently drop on the fuel assembly bundles standing in the grid plate. In such case, the dropping fuel assembly hits the fixing bar first, as shown in Fig. 14. The fixing bar, which is located in the upper part of the fuel assembly, plays the role of a barrier for protecting the fuel plates from an external impact force. Most of the kinetic energy will be absorbed by the fixing bar. It is necessary to check for fractures of the fixing bar. If a fracture has occurred, an additional impact analysis on the fuel plate is necessary. If not, the subsequent impact on the fuel plates will be precluded, which means the structural integrity of the fuel plate is ensured.

It is impossible to implement the fracture mechanical analysis in an implicit analysis. Thus, only an explicit approach is utilized for this problem. The complicated modeling, which does not have an influence on the impact results, is simply modeled using a dummy model.

3.2.1 Finite Element Model

Fig. 15 shows a finite element model at the moment of impact. Since the upper part of the falling fuel assembly has nothing to do with the contact region, it is modeled using a dummy model, which has the same weight. The two fixing bars are bonded to the side plates by welding. To implement the welds into the finite element model, the additional contact condition between the fixing bar and side plate is imposed in addition to that between the

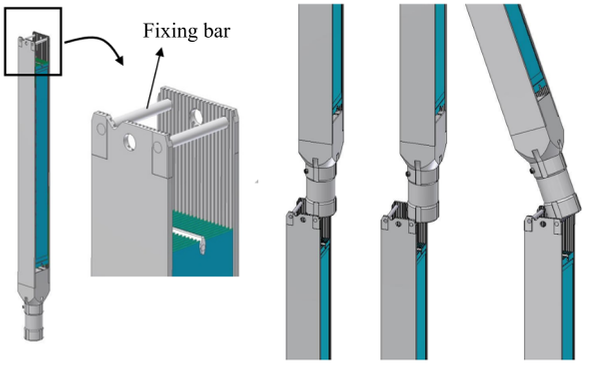

Fig. 14. Upper Part of the Fuel Assembly, and Various Impact Modes of Fuel Assembly in the Drop Accident Occurring Inside the Reactor Core

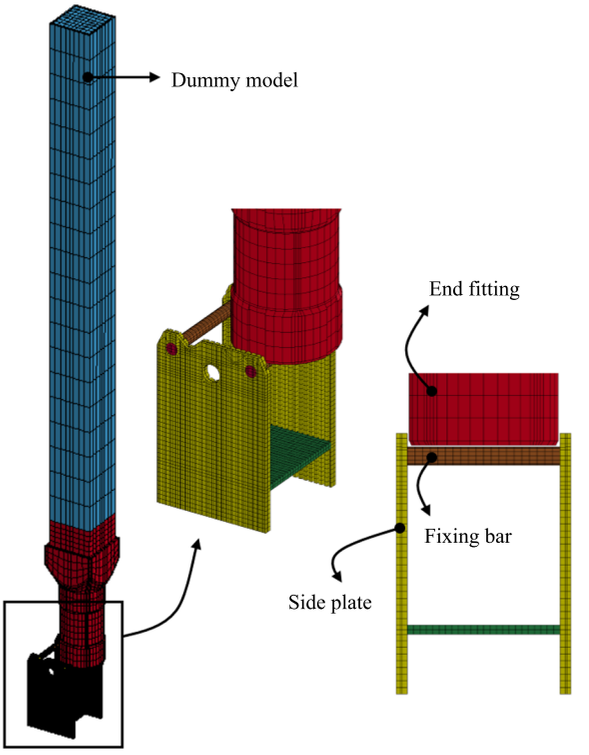

Fig. 15. Finite Element Models at the Moment of Impact

falling end fitting and fixing bar. The welding strength is assumed to be 80% of that of the base material. The dropping fuel assembly is modeled to be located just above the fixing bar of the standing fuel assembly. The impact velocity is imposed on the falling fuel assembly as initial condition. For the finite element models, 45,902 nodes and 31,562 elements are used.

To consider various impact shapes, three impact cases are considered, as shown Fig. 16. For the first case, the longitudinal axis of the end fitting is positioned on the axis of the fixing bar so that the end fitting impacts the

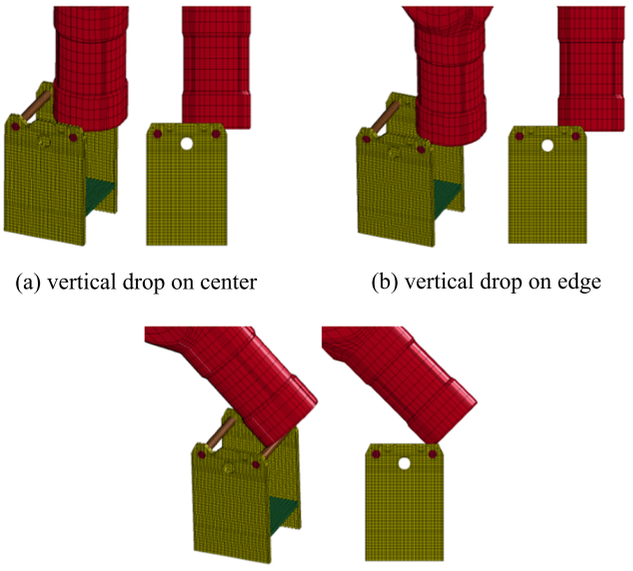

(a) vertical drop on center (b) vertical drop on edge

(c) angled drop

Fig. 16. Three Drop Cases of Fuel Assembly on Fixing Bar: Vertical Drop on Center; Vertical Drop on Edge; Angled Drop

center of fixing bar, i.e. vertical drop on center. As second drop case, the falling fuel assembly is slightly shifted so that the edge of the end fitting impacts the fixing bar, i.e. vertical drop on edge. Third case is an inclined drop, the inclined angle of which is 45°, i.e. angled drop.

3.2.2 The Analysis Results of Vertical Drop on Center

Fig. 17 shows the energy history. The total, kinetic, and internal energy of system and the fixing bar internal energy are shown. After impact, the fixing bar internal energy increases as the bar absorbs the kinetic energy of the falling fuel assembly. Fig. 18 shows the stress distribution history in which a fracture of the fixing bar has not occurred. The stress is concentrated on both ends of the fixing bar. The stress magnitude is illustrated separately in Fig. 19, in which the stress history at the middle and end points of the fixing bar are shown. The stress value is oscillated from a shock wave. Fig. 20 shows the effective plastic strain and its rate. The maximum stress and maximum effective plastic strain rate were revealed as 560.1MPa and 180 1/s, respectively. The effective plastic strain graph shows that the fixing bar undergoes plastic deformation at the moment of impact. Fig. 21 shows the contact force history. Contact force between the end fitting and fixing bar is larger than that between the side plate and fixing bar, i.e., the welding joint.

3.2.3 The analysis Results of Vertical Drop on Edge

The general behavior of second impact case, vertical drop on edge, is similar to that of first case. As in previous case, the fracture of the fixing bar has not occurred. Fig. 22 shows the stress distribution history.

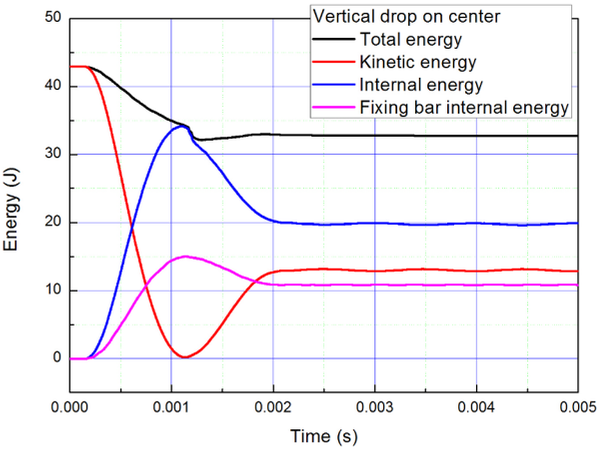

Fig. 17. Total, Kinetic, and Internal Energy Histories for Vertical Drop on Center

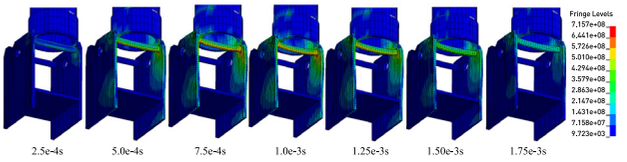

Fig. 18. Stress Distribution History for Vertical Drop on Center

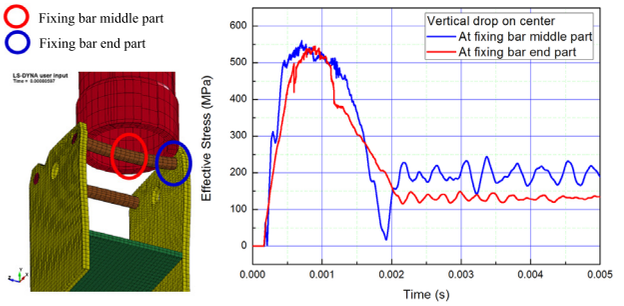

Fig. 19. Stress History of the Fixing Bar for Vertical Drop on Center

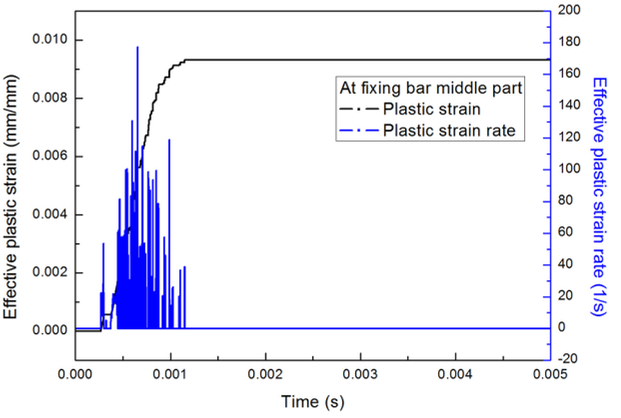

Fig. 20. Effective Plastic Strain and Plastic Strain Rate at Fixing Bar Mid-section

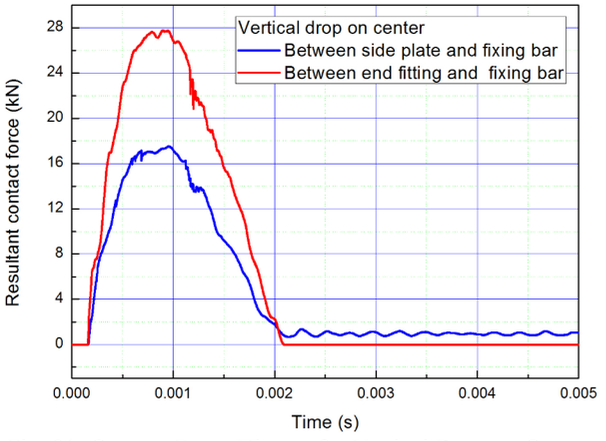

Fig. 21. Contact Force History for Vertical Drop on Center

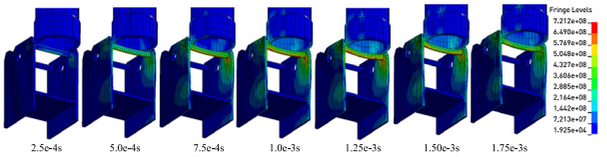

Fig. 22. Stress Distribution History for Vertical Drop on Edge

3.2.4 The Analysis Results of Angled Drop

The deformation behavior of angled drop case is a bit different from previous impact cases. It is assumed that the fuel assembly drops with an inclined angle of 45°. The impact force is imposed on the mid-section of the fixing bar with an inclined angle, which leads to the fixing bar vibrating up and down. After that, the side plates begin to vibrate in the lateral direction owing to the impulse delivery from the fixing bar, which is illustrated in Fig. 23. Fig 24 shows the history of total energy, kinetic energy, internal energy, and fixing bar internal energy. After 0.004s, the kinetic, internal energy curves are oscillated owing to the vibration behavior of the components. The history of contact forces is shown in Fig. 25. The contact force at the welded joint is larger than that between the falling end fitting and fixing bar. It is shown that the contact force at the welded joint is oscillated even after the falling fuel assembly rebounds. The fracture of the fixing bar has not occurred for angled drop.

4. CONCLUSIONS

In this study, an overall analysis approach of a fuel assembly drop accident in a research reactor was presented. The drop accidents were classified into two accident occasions based on where the accident may occur, and a numerical simulation of each accident was carried out using a finite element analysis.

For an accident occurring outside the reactor, a direct drop of the fuel assembly on the pool bottom is considered to be the most conservative case. Two different analysis schemes, implicit and explicit, were used and their results compared. The maximum stress of the fuel cladding is lower than the design limits, leading to the conclusion that the fuel structural integrity can be maintained and the fission gas release can be precluded.

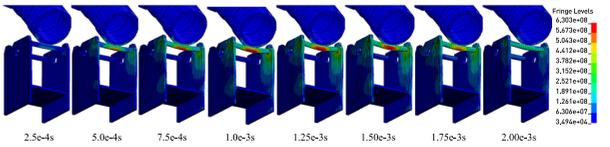

Fig. 23. Stress Distribution History for Angled Drop

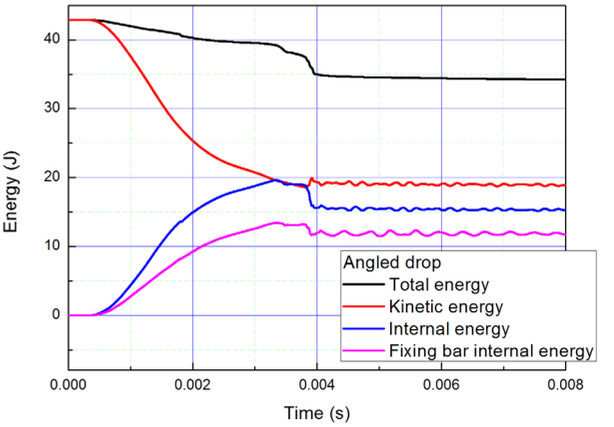

Fig. 24. Total, Kinetic and Internal Energy Histories for Angled Drop

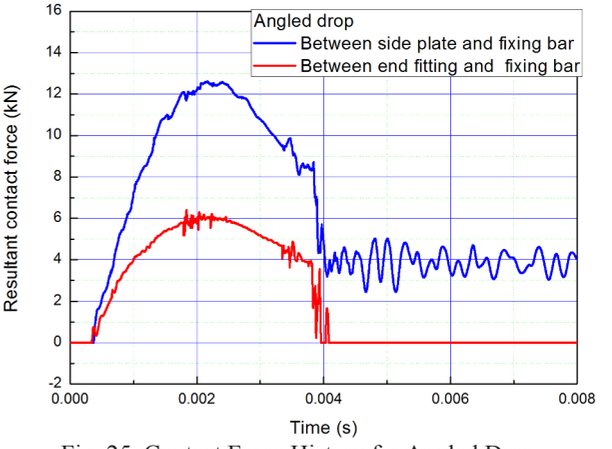

Fig. 25. Contact Force History for Angled Drop

For an accident occurring inside the reactor, the fracture of the fixing bar at the top of the standing fuel assembly is of greatest concern. In this regard, the fracture of the fixing bar is investigated under various impact cases. It was observed that no failure or fracture of the fixing bar was occurred by an impact from a dropping fuel assembly, which means the falling fuel assembly cannot impact directly on the fuel plates of the fuel assemblies standing on the core.

Through this analysis, the suitability of the analysis procedure for a fuel assembly drop impact associated with the drop situations in a research reactor is shown.

REFERENCES

[1] International Atomic Energy Agency, "Accident Analysis for Nuclear Power Plants", IAEA Safety Reports Series, No. 23, Vienna (2002)

[2] International Atomic Energy Agency, "Safety of Research Reactors", IAEA Safety Standards Series, No. NS-R-4, Vienna (2005)

[3] H.J. Wu, C.C. Tseng, and S.C. Cheng, "A Numerical Analysis for a BWR Fuel Assembly Drop Event", *J. Nucl. Sci. Technol.*, vol. 43, pp. 1068-1073 (2006).

[4] I. Namgung, S.H. Jeong, D.H. Lee, T.S. Choi, "KSNP+ Reactor Vessel Head Drop Analysis for a 5.5M Free Fall", *J. Mech, Sci, Technol.*, vol. 19, pp. 51-60 (2005)

[5] P. Petkevich, V. Abramov, V. Yuremenko, V. Piminov, V. Makarov and A. Afanasiev, "Simulation of the nuclear fuel assembly drop test with LS-Dyna", *Nucl. Eng. and Des.*, vol. 269, pp. 136-141 (2014)

[6] J.S. Yim, H.J. Kim, Y.W. Tahk, J.Y. Oh and B.H. Lee, "Evaluation of Fuel Plate Integrity during a Fuel Assembly Drop Accident Using an Energy Method", *Proc. Int. Meeting on Reduced Enrichment for Research and Test Reactors*: (RERTR 2012), Poland, Oct. 14-17, 2012.

[7] ANSYS LS-DYNA User's Guide, release 14, ANSYS INC., Southpointe, 275 Technology Drive, Canonsburg, PA 15317, USA (2011)

[8] ANSYS Structural Analysis Guide, release 14, ANSYS INC., Southpointe, 275 Technology Drive, Canonsburg, PA 15317, USA (2011).

[9] U.S Nuclear Regulatory Commission, "Safety Evaluation Report related to the Evaluation of Low-Enriched Uranium Silicide-Aluminum Dispersion Fuel for using in Non-Power Reactors," NUREG-1313 (1988)

[10] Nuclear Safety and Security Commission Notice 2012-11, Korea (2012).

[11] ASME Boiler and Pressure Vessel Code, Section III, The American Society of Mechanical Engineers (2004).

[12] R.H.J. Sellin, R.T. Moses, *Drag Reduction in Fluid Flows*: *Techniques for Friction Control*, Ellis Horwood Ltd., England (1989)

[13] D. Hasanloo, H. Pang, G. Yu, "On the Estimation of the Falling Velocity and Drag Coefficient of Torpedo Anchor during Acceleration," Ocean Eng., vol. 42, pp. 135-146 (2012).

[14] Sighard F. Hoerner, *Fluid-Dynamic Drag*, Brick Town, N.J., USA (1965)

[15] P. Wriggers, "Computational Contact Mechanics", John Wiley & Sons Ltd. Chichester (2002).

[16] G.R. Cowper and P.S. Symonds, "Strain Hardening and Strain Rate Effects in the Impact Loading of Cantilever Beams", Brown Univ. Applied Mathematics Report, pp. 28 (1958).

[17] P. Ludwik, *Element der technologischen Mechanik*, Springer (1909).